Chen, C., Buhl, E., Xu, M., Croset, V., Rees, J. S., Lilley, K. S., Benton, R., Hodge, J. J. L., & Stanewsky, R. (2015). *Drosophila* Ionotropic Receptor 25a mediates circadian clock resetting by temperature. *Nature*, *527*(7579), 516-520. https://doi.org/10.1038/nature16148

Title: *Drosophila* Ionotropic Receptor 25a mediates circadian clock resetting by temperature

Authors: Chenghao Chen[1a], Edgar Buhl[2a], Min Xu[1], Vincent Croset[4,+], Johanna S. Rees[3], Kathryn S. Lilley[3], Richard Benton[4], James J. L. Hodge[2], and Ralf Stanewsky[1*]

[a] both authors contributed equally

Affiliations:

[1] Department of Cell and Developmental Biology, University College London, 21 University Street, London, WC1E 6DE, UK.

[2] School of Physiology and Pharmacology, University of Bristol, University Walk, Bristol, BS8 1TD, UK.

[3] Cambridge Centre for Proteomics, Department of Biochemistry and Cambridge Systems Biology Centre, University of Cambridge, Tennis Court Road, Cambridge, CB2 1QW, UK.

[4] Center for Integrative Genomics, Faculty of Biology and Medicine, University of Lausanne, CH-1015 Lausanne, Switzerland.

[+]Present address: Centre for Neural Circuits and Behaviour, University of Oxford, Mansfield Road, Oxford, OX1 3SR, UK.

*Correspondence to:

Ralf Stanewsky

Tel: +44(0)20-7679-6610

Email: r.stanewsky@ucl.ac.uk

Summary:

Circadian clocks are endogenous timers adjusting behaviour and physiology with the solar day[1]. Synchronized circadian clocks improve fitness[2] and are crucial for our physical and mental wellbeing[3]. Visual and non-visual photoreceptors are responsible for synchronizing circadian clocks to light[4,5], but clock-resetting is also achieved by alternating day and night temperatures with only 2°-4°C difference[6-8]. This temperature sensitivity is remarkable considering that the circadian clock period (~24 h) is largely independent of surrounding ambient temperatures[1,8]. Here we show that *Drosophila* Ionotropic Receptor 25a (IR25a) is required for behavioural synchronization to low-amplitude temperature cycles. This channel is expressed in sensory neurons of internal stretch receptors previously implicated in temperature synchronization of the circadian clock[9]. IR25a is required for temperature-synchronized clock protein oscillations in subsets of central clock neurons. Extracellular leg nerve recordings reveal temperature -and IR25a-dependent sensory responses, and IR25a mis-expression confers temperature-dependent firing of heterologous neurons. We propose that IR25a is part of an input pathway to the circadian clock that detects small temperature differences. This pathway operates in the absence of known 'hot' and 'cold' sensors in the *Drosophila* antenna[10,11], revealing the existence of novel periphery-to-brain temperature signalling channels.

Main Text:

In *Drosophila*, daily activity rhythms are controlled by a network of ~150 clock neurons expressing the clock genes *period* (*per*) and *timeless* (*tim*). These encode repressor proteins that

negatively feedback on their own promoters resulting in 24 h oscillations of clock molecules. Temperature cycles (TC) synchronise molecular clocks present in peripheral appendages in a tissue-autonomous manner[9,12], while synchronization of clock neurons in the brain largely depends on peripheral temperature receptors located in the chordotonal organs (ChO) and the ChO-expressed gene *nocte*[9,12,13].

To discover novel factors involved in temperature entrainment, we identified NOCTE-interacting proteins by co-immunoprecipitation and mass-spectrometry (Extended Data Tab. 1)[14]. We focused on IR25a, a member of a divergent subfamily of ionotropic glutamate receptors and verified the interaction by co-immunoprecipitation after overexpressing IR25a and NOCTE in all clock cells using *tim-gal4* (Extended Data Fig. 1a). IR25a is expressed in different populations of sensory neurons, including those in the antenna and labellum[15-17]. In the olfactory system IR25a acts as a co-receptor with different odour-sensing IRs[15].

To investigate if *IR25a* is co-expressed with *nocte* in ChO we analysed *IR25a* expression in femur and antennal ChO using an *IR25a-gal4* line[15] (Extended Data Fig. 2a). *IR25a-gal4* driven *mCD8-GFP* labelled subsets of ChO neurons in the femur, overlapping substantially with *nompC-QF* driven *QUAS-Tomato* signals (Fig. 1 a-c). *nompC-QF* is expressed in larval ChO[18] and in the adult femur ChO (Fig. 1d, e). Comparison of *IR25a*-driven *mCD8-GFP* and nuclear *Ds-Red* signals with those of other ChO neuron drivers (*F-gal4* and *nocte-gal4*[9]) suggests that *IR25a* is expressed in a subset of femur ChO neurons and Johnston's Organ (JO) neurons (Fig. 1c, Extended Data Fig. 1b-g). To determine if *IR25a-gal4* ChO signals reflect endogenous IR25a expression, we confirmed the presence of *IR25a* mRNA in the femur and leg (Extended Data Fig. 2b, e) and the co-localisation of anti-IR25a immunofluorescence signals in femur ChO neurons (Fig. 1f, g).

IR25a was detected in ChO neuron cell bodies and ciliated dendrites, as was a mCherry-IR25a fusion protein expressed in these cells (Fig. 1h).

Since *nocte*^{1} mutants do not synchronize to 16°C:25°C TC in constant light (LL)[9,12] (Extended Data Fig. 3a), we analysed *IR25a*$^{-/-}$ mutants[16] under these conditions. Unlike *nocte*^{1}, the *IR25a*$^{-/-}$ flies synchronized well to this regime and we obtained similar results at warmer TC (Extended Data Fig. 3a). To test whether *IR25a* is specifically required for synchronization to small temperature intervals[7,13], we subjected *IR25a*$^{-/-}$ flies to various TC with an amplitude of only 2°C. Surprisingly, and in contrast to wild-type, *IR25a*$^{-/-}$ mutants did not synchronize to any of the shallow TC in LL or constant darkness (DD) (Fig. 2a-e, Extended Data Fig. 3b, 4c). In LL, wild-type and *IR25a* rescue flies showed a clear activity peak in the second part of the warm period before and after the 6 h shift of the TC. By contrast, *IR25a*$^{-/-}$ mutants were constantly active throughout the TC, apart from a short period of reduced activity at the beginning of the warm phase of TC1 (Fig. 2a, Extended Data Fig. 3b). In DD, control flies slowly advanced (or delayed) their evening activity peak during phase-advanced (or delayed) TC (Fig. 2b, Extended Data Fig. 4c). The phase of this activity peak was maintained in the subsequent free-running conditions (DD, const. 25°C) indicating stable re-entrainment of the circadian clock (Fig. 2b, Extended Data Fig. 4). By contrast, *IR25a* mutants did not shift their evening peak during the TC, keeping their original phase throughout the experiment (Fig. 2b, Extended Data Fig. 4c).

To quantify entrainment in LL, we determined the 'Entrainment Index' (EI)[13], whereas for most DD experiments we calculated the phase difference of the main activity peak upon release into constant conditions between *IR25a* mutants and controls. In all 2°C-amplitude TC tested the EI of *IR25a*$^{-/-}$ flies was significantly lower and phase calculation indicated no, or a significantly

reduced phase shift compared to controls (Fig. 2c-e). The same non-synchronization phenotype was observed in *IR25a*$^{-}$*/Df(IR25a)* flies, and temperature synchronization was fully restored in *IR25a*$^{-/-}$ rescue flies (Fig. 2a-d, Extended Data Fig. 3b). *IR25a*$^{-/-}$ mutants synchronize to light and have normal free-running and temperature compensated periods (Fig. 2b, Extended Data Fig. 4d, Extended Data Tab. 2). These results suggest that IR25a enables the circadian clock to sense subtle temperature changes across the entire physiological range, rather than mediating synchronization to a specific range. Consistently, increasing the TC amplitude to 4°C restored temperature entrainment in *IR25a*$^{-/-}$ flies (Extended Data Fig. 4a, b).

Temperature receptors located in fly antennae and arista are not required for temperature-synchronized behaviour[9,11,19]. As expected, we found that antennal *IR25a* function (Extended Data Fig. 1c, 2a)[16] is not required for temperature entrainment (Extended Data Fig. 5). To reveal the importance of IR25a expression in ChO neurons, we performed tissue-specific *IR25a* RNAi using validated transgenes (Extended Data Fig. 2d, 6a). *IR25a* RNAi in all or subsets of ChO neurons (Fig. 1, Extended Data Fig. 1) resulted in a lack of entrainment (Extended Data Fig. 2e, 6b, c). By contrast, *IR25a* RNAi in multidendritic, TRPA1-expressing, or clock neurons did not impair temperature entrainment (Extended Data Fig. 6c). These findings are consistent with the absence of *IR25a* expression in clock neurons and the brain (Extended Data Fig 2e-g) and show that *IR25a* functions in ChO neurons for temperature entrainment to 25°C:27° TC in LL.

To identify the neural substrates underlying the lack of behavioural synchronization, we quantified clock protein levels in wild-type, *IR25a*$^{-/-}$, and *IR25a*$^{-/-}$ *rescue* flies exposed to shallow TC in LL. While TIM expression was robustly rhythmic and synchronized in all clock neuronal groups in controls, TIM was barely detectable in the Dorsal Neuron 1 (DN1) and DN2 of *IR25a*$^{-/-}$

flies (Fig. 3a, Extended Data Figure 7a, b). Moreover, in the small and large ventral Lateral Neurons (s-LNv and l-LNv), TIM expression exhibited an additional peak during the warm phase (Fig. 3a, Extended Data Figure 7a, b). In the DN3 TIM declined earlier compared to controls and there was no effect on the dorsal Lateral Neurons (LNd). In TC and DD TIM levels in DN1 were also blunted, but oscillations in the DN2 and DN3 were similar to controls. In contrast to LL TIM was not oscillating in the s-LNv and l-LNv and at constantly low levels (Fig 3b), consistent with the behavioural results obtained under these conditions (Fig 2b, d). The alterations of TIM expression are temperature specific, as we observed normal oscillations in LD cycles at 25°C (Extended Data Fig. 7c). An increase of the TC amplitude to 4°C also restored normal TIM expression in *IR25a*$^{-/-}$ flies, in agreement with the behavioural rescue (Extended Data Figs. 7d, 4a, b). In summary, in low amplitude TC IR25a is required for normally synchronized TIM oscillations in DN1-3 and LNv in LL and in DN1 and LNv clock neurons in DD.

We tested if the clock neurons affected by the lack of IR25a are indeed involved in regulating behavioural synchronization to shallow TC by blocking synaptic transmission using tetanus-toxin (TNT). Indeed, TNT-expression in DN1 and DN2 blocked synchronization in LL, whereas in DD only DN1 blockage interfered with temperature entrainment (Fig. 3c, d)[20]. Consistent with the differential effect on TIM oscillations in LL and DD (Fig. 3a, b) these results strongly suggest that IR25a is required for the synchronized output of the DN1 (LL and DD) and DN2 (LL) to control temperature-entrained behaviour.

Next, we asked if ChO might directly sense temperature in an IR25a-dependent manner. We recorded leg nerve activity in restrained preparations and identified ChO units in the compound signal (Fig. 4a). In both wild-type and *IR25a*$^{-/-}$ flies, spontaneous leg movement changed as a

function of temperature along with motor and sensory activity. Additionally, presumed ChO activity of wild-type flies also increased during periods without movement (Fig. 4b, third insert). This temperature-induced, but movement-independent, ChO activity was absent in *IR25a*$^{-/-}$ flies showing that temperature is sensed in the legs in an IR25a-dependent manner (Fig. 4c). To test if IR25a contributes directly to temperature-sensing, we ectopically expressed this channel in the physiologically well-characterized, IR25a-negative, l-LNv (Extended Data Fig. 2f). As a positive control, we also expressed the temperature sensitive *Drosophila* TRPA1 channel[21] in the l-LNv. Isolated brains were exposed to a temperature ramp and spike frequency of individual l-LNv was recorded. Control l-LNv did not show a significant temperature-dependent change in neural activity (Fig. 4d). As expected, the firing rate of TRPA1 expressing neurons drastically increased linearly with temperature, as did other cellular parameters (Extended Data Fig. 8). *IR25a* expression resulted in linear and reversible temperature-dependent increase in action potential firing frequency (Fig 4e, i), whereas other cellular parameters showed no difference (Fig. 4f-h). Increasing the temperature by only 2-3°C also lead to a reversible increase in firing frequency of 1.03±0.20 Hz in *IR25a* expressing l-LNv (Fig. 4j). By contrast, expression of the related, but olfactory-specific co-receptor *IR8a* (which is not required for temperature entrainment, Fig. 2c) did not confer temperature-sensitivity (Extended Data Figure 8). These observations suggest that IR25a is at least part of a thermosensory receptor required for temperature entrainment.

Our data indicating that IR25a contributes to temperature sensing within ChO extend the roles of IR's beyond chemoreception, reminiscent of the requirement for the "gustatory receptor" Gr28b in warmth-avoidance[22]. Although we show that IR25a-expressing leg neurons are

capable of sensing temperature and mediating temperature entrainment, it is possible that this receptor has a similar role elsewhere in the peripheral nervous system. IR25a responds to small temperature changes and we propose that the fly continuously integrates temperature signals received from multiple ChO across the whole body for synchronization of the clock. This potential reliance on weakly responding temperature receptors might explain why the *Drosophila* circadian clock is insensitive to brief temperature pulses[23], which could help maintain synchronized clock function in natural conditions of rapid and large temperature fluctuations.

Acknowledgments:

We thank Patrick Emery, Joerg Albert, James Jepson, Paul Garrity, and Aravinthan Samuel for discussions and sharing of unpublished results, Jaga Giebultowicz for anti-TIM antibodies, Joerg Albert and James Jepson for fly stocks, Camille Tardieu and Ryan Kavlie for help with qPCR, Derek Carr for assistance with the temperature recording setup, and Maite Ogueta-Gutierrez for help with Figure preparations. The drawing for Figure 4a was generated by Polygonal Tree (http://polygonaltree.co.uk/). This work was supported by BBSRC grants BB/H001204 to R.S., BB/J0-18589/-17221 to R.S. and J.H., and a CSC PhD fellowship to C.C. V.C. was supported by a Boehringer Ingelheim Foundation Fellowship. Research in R.B.'s laboratory was supported by European Research Council Starting Independent Researcher and Consolidator Grants (205202 and 615094). MS analysis was supported by Wellcome Trust grant 099135/Z/12/Z.

Author Contributions C.C., E.B., R.S., J.H., R.B. and K.S.L. conceived, designed, and supervised the project. C.C., E.B., M.X., V.C., and J.S.R. performed experiments. C.C., E.B., and J.S.R. analysed data, and R.S. wrote the paper, with feedback from all authors.

Author Information The authors declare no competing financial interests. Correspondence and requests for materials should be addressed to R.S. (r.stanewsky@ucl.ac.uk).

Fig. 1. IR25a is expressed in ChO neurons. **a,** Overview of the femur ChO adapted from[13]. **b, d,** Double labelling of the femur ChO by *IR25a-gal4* (**b**) and *F-gal4* (**d**) driven mCD8-GFP and *nompC-QF* driven *QUAS-Tomato*. **c, e**, higher magnification of circled areas in (**b**). **f,** IR25a immunolabeling of femoral ChO cryosections of *IR25a-gal4/UAS-mCD8-GFP* flies. From left to right, GFP, anti-IR25a, 22C10, and merged images are shown. **g,** anti-IR25a and 22C10 labelling of femur ChO sections of *IR25a*$^{-/-}$ flies. **h,** Subcellular distribution of an mCherry-IR25a fusion protein co-labelled with the dendritic cap marker nompA-GFP in the femur ChO. Scale bar = 20µm.

Fig. 2. *IR25a* is required for temperature synchronization to low-amplitude temperature cycles. **a,** Upper part shows double plotted average actograms depicting the daily activity levels and environmental conditions during the entire experiment. White areas: LL and 25°C; orange areas: LL and 27°C. Histograms show daily average activity levels during the initial LL treatment and the last 3 days of each TC. Light orange: 25°C, dark orange: 27°C, white bars: activity levels

in LL. Error bars indicate s.e.m., numbers in the upper right corner 'n', x-axis: Zeitgeber time (h) and y-axis total activity (beam crossings/30 min). **b,** As in (**a**) but flies were initially kept in LD 25°C, before being exposed to a 7 h phase advanced TC in DD (dark histogram bars) and free-running conditions (DD and 25°C). Actogram shading as in (**a**) but grey areas indicate darkness. Green and red arrows indicate the position (phase) of the main activity peak during the final free run for control and mutant flies, respectively. **c, e,** EI values (mean ± s.e.m.) during (**c**) 25°C:27°C TC in LL (delay as in (**a**)), and as indicated in (**e**) (all delay, except 25°C:27°C: advance) (see Extended Data Fig. 3b for actograms and daily average plots. In (**c**) per^{01} and $nocte^{1}$ flies were used as negative controls. ***p<0.001, **p<0.01, n.s.: not significant, One way ANOVA followed by Bonferroni correction (**d**) Phase difference during DD and constant temperature after TC between $IR25a^{-/-}$ (n > 10 for each TC) and *y w* control (n > 9) and $IR25a^{-/-}$ rescue flies (n > 11). ****p<0.0001, ***p<0.001, **p<0.01; F-statistic (Watson-Williams-Stevens test).

Fig.3. IR25a is required for clock protein oscillations in central clock neurons **a, b,** TIM levels in clock neurons during LL (**a**) and DD (**b**) 25°C:27°C TC at the indicated time points (ZT). At least 8 brain hemispheres per time point were analysed for each genotype. Error bars indicate s.e.m. **c,** Progeny of *UAS-IMP-TNT* and *UAS-TNT* females crossed to *Clk4.1M-gal4* (DN1>, upper panel) or *Clk9M-gal4;Pdf-gal80* (DN2>, lower panel) males, were exposed to 2, 6h-delayed TC (12h 25°C:12h 27°C in LL). Left: actograms, shading as in Fig 2a. Right: EI calculations, numbers in bars indicate n. ** p<0.01; One way ANOVA followed by Bonferroni correction. **d**, Same genotypes as in (**c**) were exposed to an 8h-delayed 25°C: 12h 27°C TC in DD. Left: actograms

plotted as in Fig 2b, Right: phase difference of activity peaks during final constant conditions between controls (DN1/DN2 > *UAS-IMP-TNT,* n=9/12, respectively) and the indicated genotypes (DN1/DN2 > TNTE, n=16/10). ****p<0.0001, n.s. not significant, F-statistic (Watson-Williams-Stevens test).

Fig.4. IR25a is required for temperature-induced leg nerve responses and confers temperature sensitivity to l-LNv. **a,** Schematic of the setup **b,** Recording of a control fly leg nerve including motor and sensory axons. The first extended insert shows a discharge of presumed ChO sensory units in response to manual extension of the tibia (green bars). Heating the preparation from 20°C to 30°C (middle, red trace) lead to spontaneous leg movement with concurrent motor and sensory activity (2nd insert) but also to increased sensory firing in the absence of leg or motor activity (3rd insert), which was reversible with intact tibia extension response (4th insert) (n=9). **c,** *IR25a*$^{-/-}$ shows similar responses to tibia extension and temperature-dependent leg movement, but no sensory activity in response to elevated temperature (n=6). **d,** Whole cell current clamp recordings of control and Pdf>IR25a brains exposed to the indicated temperature ramp. **e,** Quantification of the temperature response from multiple recordings (mean, s.e.m.). (**f**) Vm, membrane potential; (**g**) Rin, input resistance; (**h**) F, spontaneous firing rate at 18°C. (**i),** temperature coefficient Q10 > 4, **p<0.01; t-test. Error bars indicate s.e.m., number in bars = n. **j,** *IR25a* expressing l-LNv also truthfully report small (2-3°C) temperature changes (n=5).

1 Dunlap, J. C., Loros, J. J. & DeCoursey, P. J. *Chronobiolgy: Biological Timekeeping*. (Sinauer Associates, Inc, 2004).

2 Ouyang, Y., Andersson, C. R., Kondo, T., Golden, S. S. & Johnson, C. H. Resonating circadian clocks enhance fitness in cyanobacteria. *Proc Natl Acad Sci U S A* **95**, 8660-8664 (1998).

3 Bechtold, D. A., Gibbs, J. E. & Loudon, A. S. Circadian dysfunction in disease. *Trends Pharmacol Sci* **31**, 191-198 (2010).
4 Helfrich-Förster, C., Winter, C., Hofbauer, A., Hall, J. C. & Stanewsky, R. The circadian clock of fruit flies is blind after elimination of all known photoreceptors. *Neuron* **30**, 249-261 (2001).
5 Hughes, S., Jagannath, A., Hankins, M. W., Foster, R. G. & Peirson, S. N. Photic regulation of clock systems. *Methods Enzymol* **552**, 125-143 (2015).
6 Brown, S. A., Zumbrunn, G., Fleury-Olela, F., Preitner, N. & Schibler, U. Rhythms of mammalian body temperature can sustain peripheral circadian clocks. *Curr Biol* **12**, 1574-1583 (2002).
7 Wheeler, D. A., Hamblen-Coyle, M. J., Dushay, M. S. & Hall, J. C. Behavior in light-dark cycles of Drosophila mutants that are arrhythmic, blind, or both. *J Biol Rhythms* **8**, 67-94 (1993).
8 Maguire, S. E. & Sehgal, A. Heating and cooling the clock. *Curr Opin Insect Sci* **7**, 71-75 (2015).
9 Sehadova, H. *et al.* Temperature entrainment of *Drosophila*'s circadian clock involves the gene *nocte* and signaling from peripheral sensory tissues to the brain. *Neuron* **64**, 251-266 (2009).
10 Florence, T. J. & Reiser, M. B. Neuroscience: hot on the trail of temperature processing. *Nature* **519**, 296-297 (2015).
11 Gallio, M., Ofstad, T. A., Macpherson, L. J., Wang, J. W. & Zuker, C. S. The coding of temperature in the Drosophila brain. *Cell* **144**, 614-624 (2011).
12 Glaser, F. T. & Stanewsky, R. Temperature synchronization of the *Drosophila* circadian clock. *Curr Biol* **15**, 1352-1363 (2005).
13 Wolfgang, W., Simoni, A., Gentile, C. & Stanewsky, R. The Pyrexia transient receptor potential channel mediates circadian clock synchronization to low temperature cycles in Drosophila melanogaster. *Proceedings. Biological sciences / The Royal Society* **280**, 20130959 (2013).
14 Rees, J. S. *et al.* In vivo analysis of proteomes and interactomes using Parallel Affinity Capture (iPAC) coupled to mass spectrometry. *Mol Cell Proteomics* **10**, M110 002386 (2011).
15 Abuin, L. *et al.* Functional architecture of olfactory ionotropic glutamate receptors. *Neuron* **69**, 44-60 (2011).
16 Benton, R., Vannice, K. S., Gomez-Diaz, C. & Vosshall, L. B. Variant ionotropic glutamate receptors as chemosensory receptors in Drosophila. *Cell* **136**, 149-162 (2009).
17 Rytz, R., Croset, V. & Benton, R. Ionotropic receptors (IRs): chemosensory ionotropic glutamate receptors in Drosophila and beyond. *Insect biochemistry and molecular biology* **43**, 888-897 (2013).
18 Petersen, L. K. & Stowers, R. S. A Gateway MultiSite recombination cloning toolkit. *PLoS One* **6**, e24531 (2011).
19 Sayeed, O. & Benzer, S. Behavioral genetics of thermosensation and hygrosensation in *Drosophila*. *Proc Natl Acad Sci U S A* **93**, 6079-6084 (1996).
20 Kaneko, H. *et al.* Circadian rhythm of temperature preference and its neural control in Drosophila. *Curr Biol* **22**, 1851-1857 (2012).
21 Hamada, F. N. *et al.* An internal thermal sensor controlling temperature preference in *Drosophila*. *Nature* **454**, 217-220 (2008).
22 Ni, L. *et al.* A gustatory receptor paralogue controls rapid warmth avoidance in Drosophila. *Nature* **500**, 580-584 (2013).
23 Busza, A., Murad, A. & Emery, P. Interactions between circadian neurons control temperature synchronization of *Drosophila* behavior. *J Neurosci* **27**, 10722-10733 (2007).

Methods:

Plasmids and germ-line transformations

To generate the *psp-flag-strep II-nocte-ha* (*FSNH*) construct, a *flag-strepII-venus-strepII (fsvs)* fragment was amplified from a *PiggyBac/P-element YFP- flag - strep II* construct of [14] using a Phusion High-Fidelity PCR kit (New England Biolabs). This 900 bp fragment was sub-cloned into *psp73* (Promega) to generate *psp73-fsvs* with Bgl II/ Xhol I sites. To introduce a *strepII* tag upstream of the NOCTE N-terminus, a 0.5kb fragment was amplified from *psp73-nocte-HA* (containing the entire *nocte* coding region fused to *ha*; Giesecke and Stanewsky, unpublished) by annealing the *strep II* tag directly using PCR. This fragment was religated back into *psp73-nocte-ha* to generate *psp-strep II-nocte-ha. A 3xflag* tag was introduced 5' of *psp73-strep II-nocte-ha* by sub-cloning the *strep II-nocte-ha* fragment into *psp-fsvs* with BstB I/ Xhol I sites replacing *venus*. To generate the *psp-flag-strep II-nocte-strep II* construct (*FSNS*), a Strep II tag was amplified and annealed 3' of *psp-nocte* (Giesecke and Stanewsky, unpublished) to generate *psp-nocte-strep II*, followed by sub-cloning into *psp-fsnh* using BstB I/Xhol I sites. *FSNH* and *FSNS* were sub-cloned into the transformation vector *pUAST* using Bgl II/ Xhol I sites, and transgenic flies were generated using classical transposase-mediated germline transformation. To generate *mCherry-IR25a*, the coding sequence of IR25a lacking the endogenous signal sequence (starting from codon 31) was PCR amplified, subcloned into *pUAST-mCherry attB* [15], and integrated into attP2. To generate the *IR25a* genomic rescue construct, the Bacterial Artificial Chromosome (BAC) CH322-32C20 [24] was integrated into attP16, and then recombined onto the $IR25a^2$ mutant chromosome. Restoration of IR25a expression by this BAC (in $IR25a^2$, *CH322-32C20*/$IR25a^2$, *CH322-32C20* animals) was verified by immunostaining with anti-IR25a

antibodies (data not shown). All constructs generated in this study were confirmed by DNA sequencing.

Fly strains

Flies were kept at 25°C or 18°C on common cornmeal-yeast-sucrose food under light: dark cycles and 60-70% humidity. As controls wild type Canton S and *y w* flies (both carrying the *ls-tim* allele) were used. The following flies used in this study were previously described or obtained from the Bloomington Stock Center: *tim-gal4:67* [25], *Clock856-gal4*[26]*, F-gal4:33-5* [27], *nocte-gal4* [9], *IR25a-gal4* [15], *gmr-gal4* (BL1104)*, Pdf-gal4*[28]*, elav-gal4; UAS-dicer* (BL25750), *UAS-dicer* (BL24646), *trpA1-gal4* (BL27593)*, nompC-gal4*[29]*, nompC-QF* (BL36346), *ppk-gal4* (BL32078), *UAS-GFP* [25], *nompA-GFP* [30], *UAS-mCherry* (BL52268), *QUAS-mtdTomato* (BL30037), *UAS-mCD8-GFP;UAS-DsRed* [9], *Pdf-RFP* [31]*, UAS-TrpA1* [21]*, UAS-IR25a* [15], *y per*^{01} *w* and *y per*^{L} *w* [32], *IR25a*$^{-/-}$: either homozygous *IR25a*^{2} or *IR25a*^{2}*/IR25a*^{1} flies, both null mutant alleles generated by gene targeting [16]*, IR25a*^{2}*, CH322-32C20/IR25a*^{2}*, CH322-32C20* [15] (outcrossed to Canton S for 6 generations and here referred to as *IR25a rescue*), *IR8a*^{1}: null allele of *IR8a* and referred to as *IR8a*$^{-/-}$ [15]*, nocte*^{1}: encodes truncated version of the NOCTE protein[9], *UAS-TNT-E* and *UAS-IMP-TNT-V1-B* (inactive) [33]. *Clk4.1M-gal4* and *Clk9M-gal4;Pdf-gal80* flies were used to direct GAL4 expression to subsets of the DN1p and to the DN2, respectively [20,34]. *IR25a-RNAi* lines 15627-R1 and 15627-R2 were obtained from the NIG-FLY Stock Center. *w*^{1118}; *Df(2L)Exel6010*/*CyO* was used as *IR25a* deficiency (BL7496).

Immunostaining and quantification

GFP and/or RFP signals were analysed as described in[9]. Briefly, antennae and legs were fixed and dissected in 4% paraformaldehyde/PBS solution. Samples were then washed 3 times in 3% PBST at room temperature followed by mounting in Vectashield (Vector Labs) medium and inspected using a Leica TCS SP5 confocal microscope. To visualize endogenous IR25a expression in the ChO of fly antennae and legs, cryosections (16µm) and immunolabelling were performed as described in [35] with minor modifications: sections were collected on slides and fixed for 10 min in 4% formaldehyde in PBS. After washing for 2 x 10 min in PBS, sections were treated for 30min in PBS + 0.1% Triton X-100 (PBT) and incubated in 5% normal goat serum (NGS) for 30 min. Primary antibodies (Rabbit anti-IR25a 1:500 [16], mouse anti-22C10 1:200, DSHB) were diluted in PBT with NGS and applied to slides placed horizontally in humidified chambers and left for 2 h at room temperature followed by incubation overnight at 4°C. After washing for 3 x 10 min in PBT, slides were blocked in PBT with NGS for 30 min and incubated with secondary antibodies (Rabbit AlexaFlour-594, 1:500, Mouse AlexaFlour-647 1:500, Invitrogen) diluted in PBT in the dark for 4 h at room temperature. Slides were washed 3 x 5 min in PBS and mounted in Vectashield before observation. Immunostaining of whole-mounted brains was performed as described in [36] with minor modifications. For LD experiments, flies were fixed on the 5th day of light entrainment. For temperature experiments, flies were first reared in LL and 25°C for 3 days, and then transferred to a 25°C:27°C or 25°C:29°C TC for 7 days. Therefore, the conditions are consistent with those for behavioural analysis. For temperature entrainment in DD, flies were initially entrained to LD at 25°C for 2 days followed by a 25°C:27°C TC in DD that was shifted 8 h in advance with respect to the previous LD cycle. Brains were dissected on day 6 of the TC at the indicated time points. Primary rat anti-TIM (1:1000) [37], and secondary rat

AlexaFluor-594 antibodies (Invitrogen, 1:500) were applied. Mounted brains were scanned using a Leica TCS SP5 confocal microscope. Quantification of TIM signals was performed as in [38] with minor modifications: Pixel intensity of stained neurons and background staining in each neuronal group was measured using Image J. Background signal was determined by taking the average signal of two surrounding fields of each neuronal group and was subtracted from the neuronal signal. For each group of clock neurons, at least 8 hemispheres from each genotype were checked and measured per time point. Data were normalized by setting the peak value to 1 and the ratio from each time point was then divided by the peak value.

Co-immunoprecipitation

Co-immunoprecipitation experiments were performed as described [14]. For each protein purification, 200-300 mg wet-weight of heads from *gmr-gal4* flies expressing *UAS-nocte-flag* (*FSNS* and *FSNH* transgenics were used in 2 independent experiments) or *gmr-gal4* alone (negative controls) were collected on dry ice and manually homogenized with a 2 ml Dounce homogenizer (Fisher) in 1 ml of extraction buffer (final protein concentration 5mg/ml extraction buffer) containing 50 mM Tris, pH 7.5, 125 mM NaCl, 1.5 mM $MgCl_2$, 1mM EDTA, 5% Glycerol, 0.4% NP-40, and 0.1% Tween 20. To prevent degradation during the lengthy purification steps, 2x protease mini EDTA inhibitor mixture (Roche) was added at hourly intervals throughout the procedure. The homogenate was centrifuged at 10,000 rpm for 15 min to isolate the soluble fraction used for pull-down. For the FLAG pull-down procedure, EZview™ Red ANTI-FLAG® M2 affinity gel (Sigma) was used to bind the FLAG tagged bait and its bound partners. 50µl pre-washed 50% slurry was added to 1 ml soluble protein and incubated at 4°C for 2 h on a rotary

mixer. Non-binding material was removed by centrifugation (8,000×g for 2 min) and the resin was washed three times in ice cold extraction buffer. For checking the interaction with IR25a (Extended Data Fig. 1a), the washed resin was directly boiled with 5xSDS loading buffer followed by routine Western blot. For elution the isolated protein complexes, FLAG tagged protein with any associating proteins, was incubated and eluted three times each with 50µl (100µg/ml) FLAG peptide (Sigma) in extraction buffer for 30 min at 4°C on a rotary mixer. The three eluates were combined and any residual resin was removed by centrifugation at 8,000×g for 2 min. The following mass spectrometry peptide sequencing was performed by Cambridge Centre for Proteomics. Briefly, eluates from the tagged line and untagged control flies, were processed as described [14]. The only deviation from the method described was that peptides were applied to a 180 µm x 20 mm (5 µm particle size) C18 trap column (Waters UPLC Trap Symmetry) coupled to a nanoAcquity UPLC system (Waters) using 0.1% formic acid in water (Buffer A) at a flow rate of 10 µl/min. Peptides were then separated on a 75 µm x 250 mm (1.7 µm particle size) reverse phase BEH C18 analytical nano-column (Waters) at a flow rate of 300 nl/min using a gradient of buffer A and buffer B (0.1% formic acid in acetonitrile). The HPLC system was directly coupled to a LTQ Orbitrap Velos (Thermo Scientific) with a New Objective nanospray ionisation source operated at a resolution of 60,000. Peptides were eluted with a linear gradient of 5 – 45% buffer B over 45 min or with a re-equilibration step, giving total running times of 60 min. The Orbitrap analyser survey scan was performed over a mass range of m/z 380 - 1500 each of them triggering 10 MS2 LTQ acquisitions of the 10 most intense ions exceeding 500 counts using a data dependent acquisition mode.

Western blot

For confirming the interaction between NOCTE and IR25a total head proteins were isolated from flies expressing IR25a, or IR25a and FLAG-tagged NOCTE, under the control of *tim-gal4*. Boiled beads (after Co-IP) were loaded on SDS-PAGE gels, followed by standard Western blot. Primary rabbit anti-IR25a 1:5,000 [16] and mouse anti-FLAG M2 1:1,000 (Sigma), and secondary HRP-conjugated goat anti-rabbit IgG-HRP (1:10,000) and goat anti-mouse IgG-HRP (1:1,000) antibodies (Jackson) were used.

RNA isolation and RT-PCR

For RNA extractions, 30-50 flies were collected in 2 ml RNALater (Ambion) and kept at 4°C over night, and 100µl 0.1% PBST was added to help RNALater penetration. Femurs from around 200 fly legs and 50 retinas were quickly dissected in cold RNALater. Total RNA was extracted using an RNAEasy kit (QIAGEN) according to the manufacturers' instructions. Total RNA was finally eluted in RNAase free water and stored at -80°C. cDNA synthesis was performed with Reverse Transcription Reagents Kit (Applied Biosystems) in 10µl reactions using 1 µg of total RNA according to the manufacturer's instructions. To verify mRNA expression level of *IR25a* and *nocte* in fly femur ChO, dilutions of cDNA were used for PCR with the following primers: *rp49* and *nocte* [9], *IR25a* [39], followed by DNA electrophoresis on 2% agarose gels to visualize the PCR products. To test the efficiency of *IR25a* RNAi, 20 heads of 5-10 day old flies were dissected and RNA was extracted and reverse transcribed as described above. Taqman probes for *IR25a* (CatNo.4351372, ThermoFisher) and *RPL32* (CatNo.4448489, ThermoFisher) were applied to determine the amount of mRNA. For determining *IR25a* mRNA levels in different tissues, body

parts were dissected in RNA later (Ambion). 1 μg RNA was used for cDNA synthesis. Real-time assays were performed using an ABI GeneAMP PCR system 9700 using the standard program, and Ct (threshold cycle) values were applied to determine the amount of RNA in each genotype. The relative concentrations were calculated using the $2^{-\triangle\triangle ct}$ method, and RPL32 was used as control.

Behavioural analysis

Analysis of locomotor activity of 4-5 day old male flies was performed using the *Drosophila* Activity Monitor System (DAM, Trikinetics Inc). The DAM monitors, as well as an environmental monitor (Trikinetics Inc.), were located inside a light- and temperature-controlled incubator where the fly's activity was monitored for a few weeks depending on different experimental conditions. Plotting of behavioural activity and period calculations were performed using a signal-processing tool-box [40] implemented in Matlab (MathWorks). In order to quantify behaviour during temperature cycles, an updated Histogram version based on Excel (Office, Microsoft) was applied [38]. Briefly, the activity from the last two days of each TC was plotted in Excel in 30 min bins and an 'Entrainment Index' (EI = ratio of activity occurring during the 6 h window covering the main activity peak of the positive controls over the activity during the entire warm phase) was calculated. To distinguish the clock-controlled behavioural peaks from temperature response peaks, a simple smoothing filter was applied for the four activity bins during the 2 h following each temperature transition [38]. The filtered data was used for calculation, whereas the raw activity data is plotted in the histograms. The EI values plotted in all histograms represent the average EI from the TC before and after the shift except for 18°C :

20°C and 21°C : 23°C, where the EI was generated from the TC after the shift. To calculate the phase of the main activity peaks after DD and TC involving genotypes that did not show clear activity peaks during entrainment, we employed circular phase plot analysis as previously described [40,41]. In brief, the mean activity phase of the 3 consecutive days after release into constant conditions was determined for each fly of the two genotypes to be compared. An average 'vector' indicating phase coherence (length) and mean peak phase (direction) is calculated for each genotype and the two vectors are compared by an F-statistic (Watson-Williams-Stevens test). The difference in direction is plotted in hours (h) and the mean peak phase of the controls (negative or positive controls, depending on the experiment) was set to zero.

Electrophysiology

Extracellular leg nerve recording

The question if ChO in the legs would respond to temperature changes was examined using extracellular recordings in restrained intact leg preparations. Canton S w^+ flies were used as a control and $IR25a^{-/-}$ mutants were used to test if IR25a is involved in this process. In order to minimize locomotory artifacts, flies were decapitated and all legs but the left hind leg amputated. Flies were mounted ventral side up and pinned down in a Sylgard (Dow Corning, Midland, MI, USA) coated recording chamber so that the left hind leg was orientated perpendicular to the body but not immobilized (Fig. 4a). Therefore the ChO could be stimulated in vivo by moving the tibia with a fine needle. A tungsten wire electrode, sharpened to a fine point, was inserted through the cuticle in the thorax served as a reference electrode and a

similar recording electrode was placed in the coxa of the remaining leg. The final position of the recording electrode was determined by monitoring the signal it was recording and then manually extending the tibia until a response in sensory units was seen. The signal was amplified using a BioAmp extracellular amplifier, filtered (low 5 kHz, high 10 Hz), digitized (sampling frequency 10 kHz) with a PowerLab 2/20 and recorded using LabChart 7 (ADInstruments Pty Ltd, Bella Vista, NSW, Australia).

Whole cell recordings

Different genotypes were used for each group and the data pooled as there were no differences between them: control, *Pdf-RFP* and *Pdf-gal4; UAS-mCherry*; IR25a, *Pdf-gal4/UAS-IR25a; Pdf-RFP* and *Pdf-gal4/UAS-mCherry-IR25a*; TrpA1, *Pdf-gal4/UAS-TrpA1; Pdf-RFP* and *Gal1118-gal4/UAS-TrpA1/UAS-RFP*; IR8a, *Pdf-gal4/UAS-IR8a; Pdf-RFP* and *Pdf-gal4/UAS-mCherry-IR8a*. Experiments were performed under red light illumination and light exposure during dissection was kept to a minimum. For visualization of the l-LNv we used RFP-tagged constructs and a 555 nm LED light source in order to not activate cryptochrome. Adult flies raised in 12h:12h LD at 25°C, were collected ~3-5 days post eclosion between ZT13 and ZT16, decapitated and brains dissected in extracellular saline solution containing (in mM): 101 NaCl, 1 $CaCl_2$, 4 $MgCl_2$, 3 KCl, 5 glucose, 1.25 NaH_2PO_4, 20.7 $NaHCO_3$, pH adjusted to 7.2. The brains were transferred for 5-10 min to saline containing 20 U/ml papain with 1 mM L-cysteine to digest the ganglion sheath. After removal of the photoreceptors, air sacks and trachea, a small incision was made over the position of the l-LNv neurons in order to give easier access for the recording electrodes. Brains were placed ventral side up in the recording chamber, secured

using a custom-made anchor and during recordings continuously perfused with aerated (95% O_2, 5% CO_2) saline solution. l-LNv neurons were identified on the basis of their fluorescence, size and position. A single recording was performed from one l-LNv per brain. Whole cell current clamp recordings were performed using glass electrodes with 10-20 MΩ resistance filled with intracellular solution (in mM: 102 K-gluconate, 17 NaCl, 0.94 EGTA, 8.5 HEPES, 0.085 $CaCl_2$, 1.7 $MgCl_2$, pH 7.2) and an Axon MultiClamp 700B amplifier, digitized with an Axon DigiData 1440A (sampling rate: 20 kHz; filter: Bessel 10 kHz) and recorded using pClamp 10 (Molecular Devices, CA, USA). A cell was included in the analysis if the access resistance was less than 70 MΩ and the leak current in response to a -40 mV pulse less than -100 pA. All chemicals were purchased from Sigma (Poole, UK). The liquid junction potential was calculated as 13 mV and was subtracted from all the membrane voltages. Resting membrane potential (Vm) was measured after stabilizing for 2-3 min. Membrane input resistance (Rin) was calculated by injecting hyperpolarising current steps and measuring the resulting changes in voltage. Spike frequency was manually measured using 10 s bins for each degree of temperature. To test the effect of elevated temperature, the recording chamber and the perfusion influx were gradually heated from 18°C to 30°C within 5-10 min and cooled back to 18°C within 10-15 min using a Peltier heating system (ALA Scientific Instruments, NY, USA) and TC-10 controller (npi, Tamm, Germany). The temperature coefficient Q10 was calculate by dividing the firing rate at 30°C by the rate at 20°C. To check whether l-LNvs can also sense small temperature changes of 2-3°C, neurons were recorded as before, the temperature increased to around 24.5°C held for 3 min, then increased to 27.5°C held again for 3 min, cooled back down to 24.5°C and recorded for a further 3 min. During the whole period the instantaneous spiking

frequency was monitored. All values are given as mean and s.e.m. and a t-test and ANOVA (followed by Tukey test) were used to calculate significant differences.

Extended Data Figure 1. IR25a and Nocte physically interact in vivo and are expressed in femur and antennal ChO neurons. **a,** In vivo Co-IP experiments using protein extracts from fly heads. Head lysates were immunoprecipitated using anti-FLAG antibody. The immunoprecipitates were examined by Western blotting using anti-FLAG and anti-IR25a antibody. Input represents 30% of cell lysates used in the pull-down experiment. The genotypes of the flies used were: *tim > IR25a*: *UAS-GFP/UAS-IR25a; tim-gal4:67/+. tim > IR25a+FLAG-NOCTE*: *UAS-FSNH/UAS-IR25a; tim-gal4:67/+*. The bracket indicates that NOCTE-FLAG runs as a double band on Western blots. For source data, see Supplementary Figure 1. **b,** Overview of the antennal and femur ChO adapted from [13,42]. **c, d,** Labelling of the JO neurons by *IR25a-gal4* (**c**) and *F-gal4* (**d**) driven membrane bound mCD8-GFP and nuclear-localized Ds-Red expression. Note that *IR25a* is expressed in only a subset of JO neurons. **e, f,** Same flies as in (**c, d**) analysed for *IR25a* expression in the femoral ChO. Again, only subsets of the ChO neurons express *IR25a*. Arrowheads in (**c, e**) point to ChO neuron nuclei. **g,** Labelling of the ChO neurons in JO and femur by *nocte-gal4* driven membrane bound GFP and nuclear Ds-Red expression[9]. Scale bar = 20 μm.

Extended Data Figure 2. Spatial and quantitative *IR25a* mRNA and protein expression in CNS and PNS tissues and efficiency of RNAi-mediated knockdown. **a,** Analysis of *IR25a-gal4* and

IR25a in the 3rd segment of the antenna reveals expression in coeloconic sensilla[16]. Schematic adapted from[15]. **b, c,** Determination of *IR25a* and *nocte* mRNA levels in femur and retinal tissues by semi-quantitative RT-PCR; *rp49* was used as control. For gel source data, see Supplementary Figure 1. **d, e**, qPCR analysis of *IR25a* mRNA levels in whole heads (**d**), or dissected body parts (as indicated) (**e**) from flies of the genotypes indicated. Pan-neuronal *elav-gal4* knock-down (**d**) decreased *IR25a* mRNA >75%, or >90%, using one or two different RNAi lines combined, respectively. ****p<0.0001, ***p<0.001, *p<0.05, One way ANOVA followed by Bonferroni correction. **f,** IR25a is not expressed in the central brain and clock neurons. Left: IR25a immunolabelling of a Canton S brain reveals no signals. Middle: same brain labelled with anti-TIM reveals expression in clock neurons. Right: Merge. Brains were dissected in LD at ZT20. Scale bar=10 μm. **g,** *IR25a-gal4* is not expressed in clock neurons and largely absent from the brain. Left: nuclear Ds-Red driven by *IR25a-gal4*. 2nd from left: anti-PDF staining showing LNv and their projections. Middle: anti-PER (diluted 1:5000)[43] showing all clock neurons. 2nd from right: Merge, showing two *IR25a-gal4* positive cell in the antennal lobe, not co-localized with any of the clock neurons. These cells were observed in 4/8 hemispheres and always on the same side of the brain. Right: magnified view of circled area in the merged image. Scale bar = 30 μm.

Extended Data Figure 3. *IR25a* is required for temperature synchronization to low-amplitude temperature cycles but not for high-amplitude temperature cycles. **a,** Canton S, *IR25a*$^{-/-}$, and *nocte*^{1} flies were exposed to LD at 20°C for 5 days (left) or LL at 25°C for 2 days (right), followed

by exposure to a 12h : 12h 20°C : 29°C (left) or 16°C : 25°C (right) TC in LL , which after 6-7 days was delayed or advanced by 6 h, respectively. Warmer temperature indicated by red and orange shading, respectively **b,** Actograms and daily averages of Canton S and *IR25a*$^{-/-}$, and *IR25a*$^{-/-}$ flies containing a genomic *IR25a* rescue construct (*rescue*) exposed to 18°C : 20°C TC in LL (left) and 21°C : 23°C TC in LL (right). Warm phase in actograms indicated by orange shading. Histogram colour coding as in Fig. 2. For quantification see Fig. 2e.

Extended Data Figure 4. *IR25a* is not required for temperature synchronization to high- but to low amplitude TC and *IR25a*$^{-/-}$ flies show normal LD and DD behaviour. **a,** Canton S and *IR25a*$^{-/-}$ flies were exposed to LL at 25°C for 2-3 days, followed by exposure to high-amplitude 12h : 12h TC in LL, which after 5-6 days were delayed by 6 h. Double plotted average actograms depicting the daily activity levels and environmental conditions during the entire experiment are shown. Actual temperatures are colour coded and indicated below the EI calculations. numbers in bars indicate n. **b,** As in (**a**) but flies were initially kept in LD and DD for 2 days each (left) or LD (right), before being exposed to 2 phase delayed (left) or advanced (right) TC in DD at the temperatures indicated. n.s.: not significant. **c,** Behaviour of *IR25a*$^{-/-}$ and *rescue* flies during DD and 25°C : 27°C TC with 8 h delay and during DD and 21°C : 23°C TC with a 8 advance compared to the previous LD cycle (at 25°C). Warm phase is indicated by orange shading. **d,** Canton S and *IR25a*$^{-/-}$ flies during LD and DD conditions at 25°C (see Tab. S2 for period calculations).

Extended Data Figure 5. Antennal *IR25a* expression is not necessary for synchronization of locomotor activity rhythms to temperature cycles. Ablation of antennae as indicated. **a,** *IR25a*$^{-/-}$ and *rescue* flies were exposed to the same condition used in Fig. 2. Actograms and daily averages as described before. **b,** Quantification of behaviour as described in Fig. 2. The data of *IR25a*$^{-/-}$ with normal antennae was taken from Fig. 2a. n.s.: not significant.

Extended Data Figure 6. Knocking-down *IR25a* expression via RNA-interference disrupts synchronization of locomotor activity rhythms to temperature cycles (25°C : 27°C in LL). **a, b,** Behaviour of flies with spatially restricted *IR25a* knock-down mediated by *IR25a-gal4* (**a**), *ChO* specific *F-gal4,* and *nompC-gal4* (**b**) driven *IR25-RNAi* expression, respectively. Control flies are *UAS-dicer2/Y; IR25-gal4/+* (**a**), and *UAS-dicer2/Y;; F-gal4/+* or *UAS-dicer2/Y;; nompC-gal4/+* (**b**).Test flies carry the same transgenes, but in addition 1 or 2 copies of the *IR25a-RNAi* line indicated. Actograms and daily averages as described for Fig. 2a. **c,** Progeny of the respective *UAS-IR25a-RNAi* lines crossed to *y w* (left 3 columns) and flies from (**a, b**) and the other *gal4* drivers indicated, were exposed to the same LL and TC conditions used in Fig. 2a. As controls, *UAS-dicer, gal4* driver lines were crossed to *y w* and F1 males containing *UAS-dicer/Y* and the respective *gal4/+* were tested. Numbers of analysed individuals (n) are indicated above each column. Entrainment was quantified as in Fig. 2c. ****p<0.0001, One way ANOVA followed by Bonferroni correction.

Extended Data Figure 7. Rescue of TIM oscillations in clock neurons during low amplitude temperature cycles and normal TIM oscillations during LD and high-amplitude TC. **a, b,** TIM levels in clock neurons during LL 25°C : 27°C TC at the indicated time points (ZT) in the genotypes indicated. At least 8 brain hemispheres per time point were analysed for each genotype. Scale bars = 10µm. Data in (**b**) are mean ± s.e.m. **c,** Quantification of TIM levels in clock neurons during LD (25°C) in Canton S and *IR25a*$^{-/-}$ mutant brains. **d,** TIM oscillations in different clock-neuronal groups in *IR25a*$^{-/-}$ are restored in 25°C : 29°C TC in LL. At least 8 brain hemispheres per time point were analysed for each genotype and condition. Error bars indicate s.e.m.

Extended Data Figure 8. Ectopic expression and heat responses of TRPA1 and IR8a in l-LNv clock neurons. **a,** Whole cell current clamp recordings of *Pdf-gal4/UAS-TrpA1; Pdf-RFP* (top trace, red) and *Pdf-gal4/UAS-IR8a-RFP* (bottom trace, black) brains exposed to a temperature ramp from 18°C to 30°C and back to 18°C. Note the additional depolarization of the *TrpA1* neuron at higher temperatures. **b,** Compared to control (Fig. 4), recordings from *TrpA1* expressing neurons show a large increase in firing rate with temperature which the IR8a expressing neurons do not. **c, d** In comparison to control neurons (data taken from Fig. 4) the membrane potential of *TrpA1* expressing neurons is more positive at 30°C (open bars) and the input resistance is also significantly reduced in *TrpA1* at 18°C. **e, f** The firing rate at 18°C is higher for IR8a neurons but only the Q10 of *TrpA1* is different to control. Bars are means and whiskers s.e.m., n indicated in bars, * $p<0.05$, *** $p<0.001$, ANOVA followed by Tukey-test.

Extended Data Table 1. Mass Spectrometry data from fly heads from 3 different genotypes. *gmr-gal4 > UAS-Flag-Strep-Nocte-Strep* (*FSNS*), *gmr-gal4 > UAS-Flag-Strep-Nocte-HA* (*FSNH*) and control *gmr-gal4* (driver only, NEG). Data show the numbers of unique peptides, the % protein sequence coverage, Mascot Scores (Matrix Science) and EMPAI (empirical abundance index) scores and the peptides sequences derived from Mascot search engine. Data were compared using Protein Centre (Thermo). Black entries are high confidence hits and grey entries are lower confidence based on prior knowledge of known contaminants [14]. *nocte* mutants show defects in ChO morphology, pointing to a structural role of NOCTE in ChO cilia[9]. Consequently, the majority of the identified proteins (10/16) likely regulate function and dynamics of the ChO neuron cilia. Since we were mainly interested in identifying potential temperature receptors, we focused on other NOCTE-interacting proteins, particularly on Ionotropic Receptor 25a (IR25a).

Extended Data Table 2. Rhythm analysis of control and *IR25a* mutant flies under free running (DD) conditions at different ambient temperatures. Period values were calculated using autocorrelation as described in [40]. Flies with a Rhythm Statistics (RS) value > 1.5 were considered rhythmic [40].

24 Venken, K. J. *et al.* Versatile P[acman] BAC libraries for transgenesis studies in Drosophila melanogaster. *Nat Methods* **6**, 431-434 (2009).

25 Kaneko, M. & Hall, J. C. Neuroanatomy of cells expressing clock genes in *Drosophila*: transgenic manipulation of the *period* and *timeless* genes to mark the perikarya of circadian pacemaker neurons and their projections. *J Comp Neurol* **422**, 66-94 (2000).

26 Gummadova, J. O., Coutts, G. A. & Glossop, N. R. Analysis of the Drosophila Clock promoter reveals heterogeneity in expression between subgroups of central oscillator cells and identifies a novel enhancer region. *J Biol Rhythms* **24**, 353-367 (2009).

27 Kim, J. *et al.* A TRPV family ion channel required for hearing in *Drosophila*. *Nature* **424**, 81-84 (2003).

28 Park, J. H. & Hall, J. C. Isolation and chronobiological analysis of a neuropeptide pigment-dispersing factor gene in Drosophila melanogaster. *J Biol Rhythms* **13**, 219-228 (1998).
29 Liu, L. *et al.* Drosophila hygrosensation requires the TRP channels water witch and nanchung. *Nature* **450**, 294-298 (2007).
30 Chung, Y. D., Zhu, J., Han, Y. & Kernan, M. J. *nompA* encodes a PNS-specific, ZP domain protein required to connect mechanosensory dendrites to sensory structures. *Neuron* **29**, 415-428 (2001).
31 Ruben, M., Drapeau, M. D., Mizrak, D. & Blau, J. A mechanism for circadian control of pacemaker neuron excitability. *J Biol Rhythms* **27**, 353-364 (2012).
32 Konopka, R. J. & Benzer, S. Clock mutants of *Drosophila melanogaster*. *Proc Natl Acad Sci U S A* **68**, 2112-2116 (1971).
33 Sweeney, S. T., Broadie, K., Keane, J., Niemann, H. & O'Kane, C. J. Targeted expression of tetanus toxin light chain in Drosophila specifically eliminates synaptic transmission and causes behavioral defects. *Neuron* **14**, 341-351 (1995).
34 Zhang, Y., Liu, Y., Bilodeau-Wentworth, D., Hardin, P. E. & Emery, P. Light and temperature control the contribution of specific DN1 neurons to Drosophila circadian behavior. *Curr Biol* **20**, 600-605 (2010).
35 Saina, M. & Benton, R. Visualizing olfactory receptor expression and localization in Drosophila. *Methods Mol Biol* **1003**, 211-228 (2013).
36 Yoshii, T., Todo, T., Wülbeck, C., Stanewsky, R. & Helfrich-Förster, C. Cryptochrome is present in the compound eyes and a subset of *Drosophila*'s clock neurons. *J Comp Neurol* **508**, 952-966 (2008).
37 Rush, B. L., Murad, A., Emery, P. & Giebultowicz, J. M. Ectopic CRYPTOCHROME renders TIM light sensitive in the *Drosophila* ovary. *J Biol Rhythms* **21**, 272-278 (2006).
38 Gentile, C., Sehadova, H., Simoni, A., Chen, C. & Stanewsky, R. Cryptochrome antagonizes synchronization of Drosophila's circadian clock to temperature cycles. *Curr Biol* **23**, 185-195 (2013).
39 Croset, V. *et al.* Ancient protostome origin of chemosensory ionotropic glutamate receptors and the evolution of insect taste and olfaction. *PLoS Genet* **6**, e1001064 (2010).
40 Levine, J. D., Funes, P., Dowse, H. B. & Hall, J. C. Signal analysis of behavioral and molecular cycles. *BMC Neurosci* **3**, 1 (2002).
41 Simoni, A. *et al.* A mechanosensory pathway to the Drosophila circadian clock. *Science* **343**, 525-528 (2014).
42 Wilson, R. I. & Corey, D. P. The force be with you: a mechanoreceptor channel in proprioception and touch. *Neuron* **67** (2010).
43 Stanewsky, R. *et al.* Temporal and spatial expression patterns of transgenes containing increasing amounts of the *Drosophila* clock gene *period* and a *lacZ* reporter: mapping elements of the PER protein involved in circadian cycling. *J Neurosci* **17**, 676-696 (1997).

Figure 1

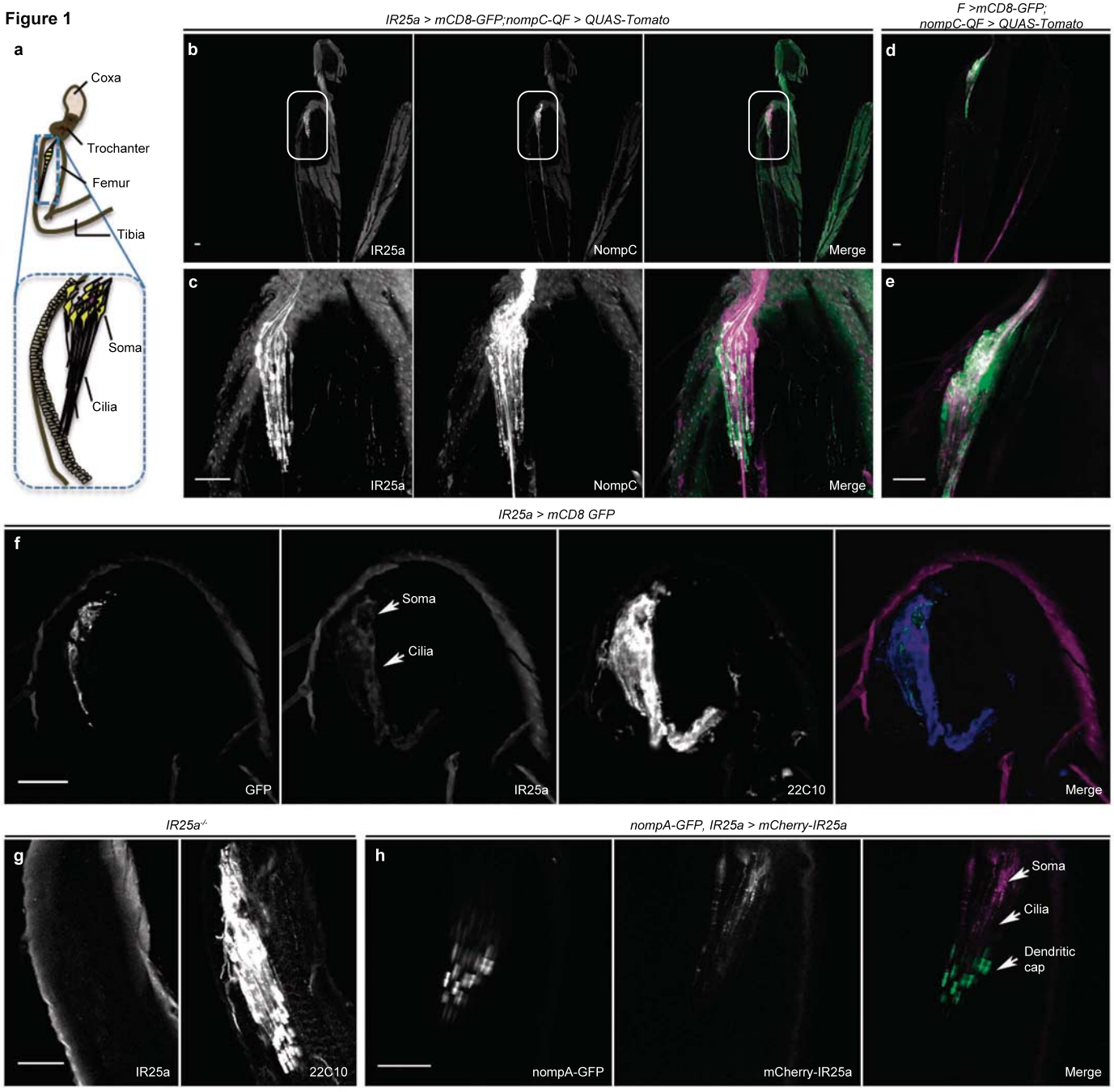
a
Coxa
Trochanter
Femur
Tibia
Soma
Cilia
IR25a > mCD8-GFP;nompC-QF > QUAS-Tomato
b
IR25a
NompC
Merge
c
IR25a
NompC
Merge
F >mCD8-GFP;
nompC-QF > QUAS-Tomato
d
e
IR25a > mCD8 GFP
f
Soma
Cilia
GFP
IR25a
22C10
Merge
IR25a-/-
g
IR25a
22C10
nompA-GFP, IR25a > mCherry-IR25a
h
nompA-GFP
mCherry-IR25a
Soma
Cilia
Dendritic
cap
Merge

Figure 2

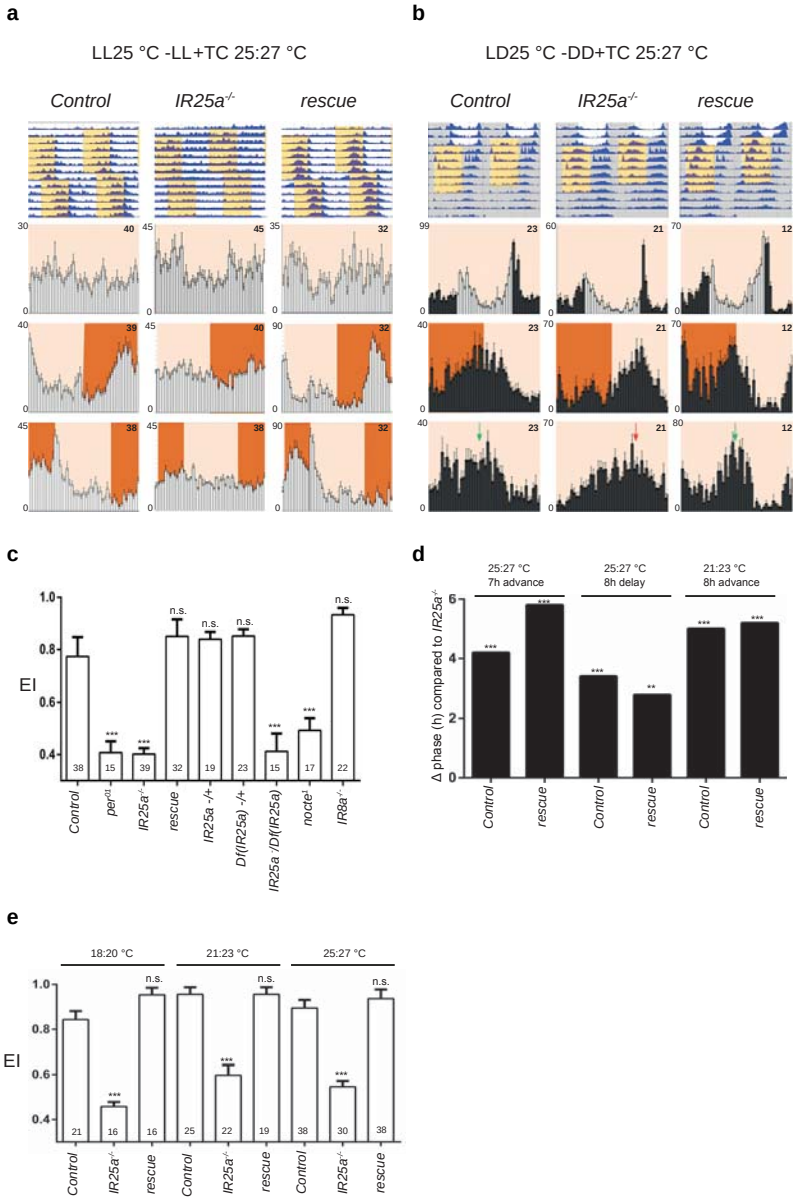
a
LL25 °C -LL+TC 25:27 °C
Control
IR25a-/-
rescue
b
LD25 °C -DD+TC 25:27 °C
Control
IR25a-/-
rescue
c
EI
n.s.
Control
per01
IR25a-/-
rescue
IR25a -/+
Df(IR25a) -/+
IR25a -/Df(IR25a)
nocte1
IR8a-/-
d
25:27 °C
7h advance
25:27 °C
8h delay
21:23 °C
8h advance
Δ phase (h) compared to IR25a-/-
Control
rescue
e
18:20 °C
21:23 °C
25:27 °C
EI
n.s.
Control
IR25a-/-
rescue

Figure 3

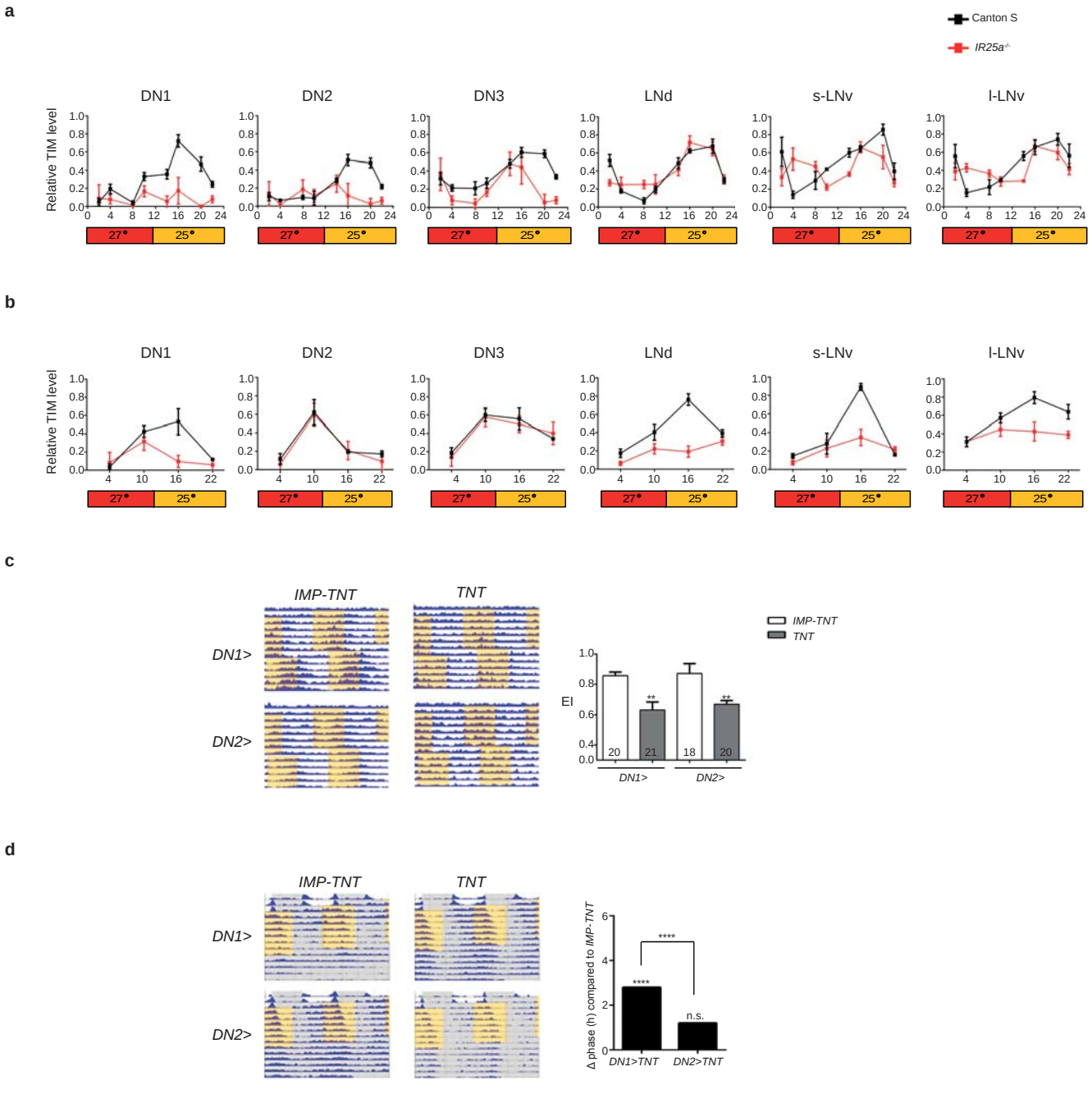
a
Canton S
IR25a-/-
DN1
DN2
DN3
LNd
s-LNv
l-LNv
Relative TIM level
27°
25°
b
c
IMP-TNT
TNT
DN1>
DN2>
EI
d
Δ phase (h) compared to IMP-TNT
DN1>TNT
DN2>TNT
n.s.

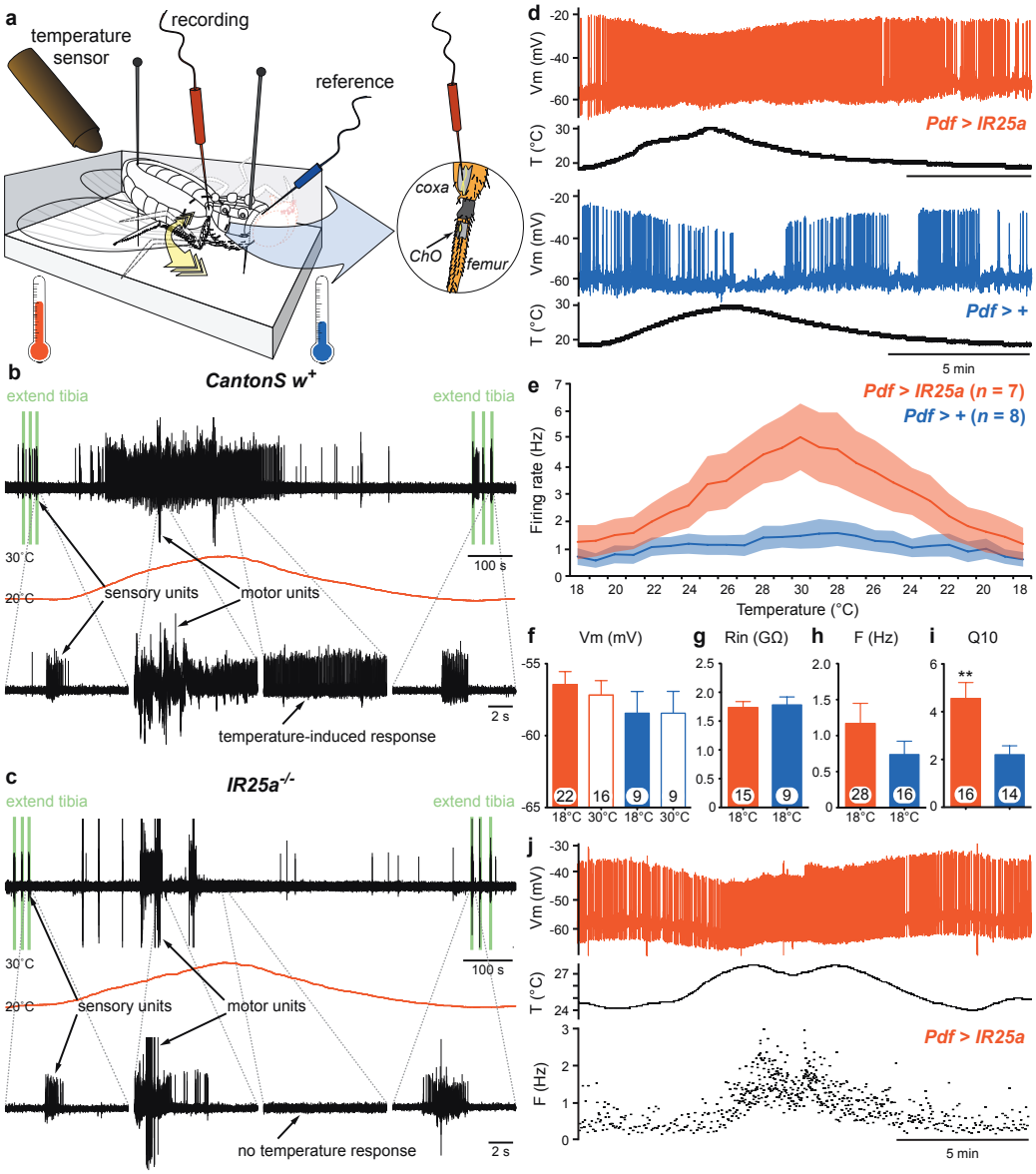
a
temperature sensor
recording
reference
coxa
ChO
femur
b
CantonS w+
extend tibia
extend tibia
30°C
20°C
sensory units
motor units
100 s
2 s
temperature-induced response
c
IR25a-/-
extend tibia
extend tibia
30°C
20°C
sensory units
motor units
100 s
2 s
no temperature response
d
Vm (mV)
T (°C)
Pdf > IR25a
Pdf > +
5 min
e
Pdf > IR25a (n = 7)
Pdf > + (n = 8)
Firing rate (Hz)
Temperature (°C)
f
Vm (mV)
g
Rin (GΩ)
h
F (Hz)
i
Q10
18°C 30°C 18°C 30°C
18°C 18°C
18°C 18°C
**
j
Vm (mV)
T (°C)
F (Hz)
Pdf > IR25a
5 min